Crop production in the Hexi Corridor challenged by future climate change

Journal Pre-proofs

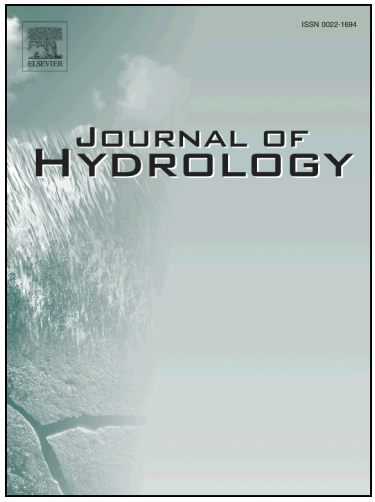

Research papers

Crop production in the Hexi Corridor challenged by future climate change

Jing Fu, Jun Niu, Shaozhong Kang, Adebayo J. Adeloye, Taisheng Du

PII: S0022-1694(19)30932-1
DOI: https://doi.org/10.1016/j.jhydrol.2019.124197
Reference: HYDROL 124197

To appear in: *Journal of Hydrology*

Received Date: 24 March 2019
Revised Date: 26 August 2019
Accepted Date: 28 September 2019

Please cite this article as: Fu, J., Niu, J., Kang, S., Adeloye, A.J., Du, T., Crop production in the Hexi Corridor challenged by future climate change, *Journal of Hydrology* (2019), doi: https://doi.org/10.1016/j.jhydrol.2019.124197

Crop production in the Hexi Corridor challenged by future climate change

Jing Fu[a,b], Jun Niu[a,b*], Shaozhong Kang[a,b], Adebayo J. Adeloye[c], Taisheng Du[a,b]

[a]*Center for Agricultural Water Research in China, China Agricultural University, Beijing 100083, China*

[b]*Wuwei Experimental Station for Efficient Water Use in Agriculture, Ministry of Agriculture and Rural Affairs, Wuwei 733000, China*

[c]*Institute for Infrastructure and Environment, Heriot-Watt University, Edinburgh EH14 4AS, United Kingdom*

SUMMARY

Drought is one of the costliest natural hazards and the main factor of concern impacting crop growth in the arid Hexi Corridor in Northwest China. However, the inter-relationship between meteorological drought severity and crop yield is seldom studied across this region. In this study, two multi-scalar drought indices: the Standardized Precipitation Index (SPI) and the Standardized Precipitation-Evapotranspiration Index (SPEI) are employed to monitor the evolution of drought condition in the Hexi Corridor. We examined (a) the historical drought evolution of the Hexi Corridor since 1970s; (b) the possible future drought tendency under different RCP scenarios; and (c) the multi-scale correlation between climatic crop yield and drought indices. The results indicate that the studied area experienced a trend towards warmer and wetter conditions during the last 4 decades and this trend last until the middle 2030s indicated by SPEI. The feasibility of SPEI and SPI for quantifying drought condition and evaluating production loss was tested in the arid and semi-arid regions of northwest of China and SPEI was found more reliable. Correlation analysis between climatic yield and drought indices revealed that the

drought condition of the month July detected by 3-month SPEI was the most relevant for the observed changes in climate yield in the Hexi Corridor. By obtaining the critical point of each SPEI-climatic yield curve, we found the different levels of yield vulnerability for the four selected districts, according to which we are able to gain an early prediction of the crop production crisis corresponding to the future drought events.

Key words: Drought; SPI; SPEI; Crop yield; Climate change

1. Introduction

Drought is an important kind of extreme events that severely damages the agriculture, ecology, water resources and human lives around the world, being one of the costliest and most widespread natural hazards (Wilhite and Glantz, 1985; Dai, 2011; Niu et al., 2015). Under the changing environment, water scarcity, which is being further compounded by droughts, is posing increasingly larger threats to the carbon cycle and food production (Sivakumar, 2011; Lesk et al., 2016). Thus, understanding the mechanism and modelling of droughts has drawn much attention from ecologists, meteorologists and agricultural scientists (Mishra and Singh, 2011; Niu and Chen, 2014; Niu et al., 2017).

Drought is apparent after a long-period lack of rainfall in a region, but the onset, duration and end of it is difficult to determine. An effective way to monitor drought condition is by utilizing drought indices. Many indices have been developed to monitor, predict and assess the severity of drought, such as the Palmer Drought Index

(PDSI), which is a landmark in the history of drought indices. The PDSI incorporates antecedent precipitation, moisture supply, and moisture demand into a hydrologic accounting system (Palmer, 1965; Richard and Heim, 2002). Multi-scalar indices have been developed to improve the existing ones such as the Standard Precipitation Index (SPI; Mckee et al., 1993) and the Standard Precipitation Evapotranspiration Index (SPEI; Vicente-Serrano et al., 2010), making the monitoring of drought more comparable both temporally and spatially. The calculation procedure of the SPI and SPEI is relatively simple compared to the existing drought indices and it has the advantage of flexible time scales, making it widely employed in droughts-related studies. The most important difference of the two indices is that SPEI is calculated using precipitation and PET (potential evapotranspiration), in other words, it considers a simple water balance in a specific area, which is particularly suited to detect the consequences of global warming on drought conditions (Vincente-Serrano et al., 2010).

Crop yield loss is one of the most devastating consequences of droughts on the water-carbon cycle . Increasing frequency of dry, hot episodes can lead to reduced yields and greater yield variability for crops, thus resulting in higher costs for farmers (Potop et al, 2010). Food security is becoming a hot spot in China due to the extensive attention to climate change. As a country with a large agriculture land, China is prone to costly drought impacts, e.g., the average area that affected by drought is up to 20,900 km^2 $year^{-1}$ and the direct economic losses are up to 32 billion Chinese yuan $year^{-1}$ over the period 1949–2013 (Zhai et al., 2014; Qin et al., 2015). Drought indices

have been reported to be widely used in the explanations of crop yield losses (Kola et al., 2014; Arshad et al., 2013; Peña-Gallardo et al., 2019) and it is proved that multi-scalar drought indices have better performance than other drought indices in identifying the impacts of drought on crop yields (Vicente-Serrano et al., 2012; Wang et al., 2016a, b). As it is difficult to get accurate long-term crop yield data, model simulated data and satellite based data are also utilized in the relevant studies (Boogaard et al., 2014). Liu et al (2015) studied the relation between PDSI and crop yield simulated by EPIC model in an agricultural region in Northwest China and found that droughts in April, July and September are more responsible for yield loss of spring and winter wheat. In recent years, statistical methods have been applied feasibly by arrange of researches (Lobell et al., 2011; Tack et al., 2015; Schauberger et al., 2017) for the flexibility and easy access.

Previous studies have investigated how drought impact on crop growth and found that drought in the earlier growing period has larger influences on crop yields. Mkhabela et al (2010) found that drought indices based on water demand are more corelated to yield and quality of Canadian prairie spring wheat than other kinds of indices and drought indices accumulated from planting to anthesis were superior to those accumulated from anthesis to maturity. Prabnakorn et al (2018) used SPEI to study the relation between drought and rice yield in the Mun River basin and found that the 1-month SPEI has stronger correlation with rice yield than other timescales and rainfall. The Hexi Corridor, located in the typical arid region of northwestern China, is an important crop production base and is very sensitive to climate change

(Niu et al., 2017). However, few studies have investigated the impact of drought on crop yield in this area. Thus, it is of great importance to investigate the current and future drought condition and study the inter-relationship between drought indices and food production in this area.

The objectives of this study are to: (1) analyze the temporal and spatial evolution of historical droughts over the period 1970–2015; (2) project future drought condition by calculating the drought indices (SPEI and SPI) form the year 2017 to 2050; and (3) investigate the relationship between drought indices and crop production and propose adaptive strategies according to the projection results.

2. Study area

The Hexi Corridor lies in the typical arid region in the northwest of China between longitudes 92°12’ and 104°20’E and latitudes 37°17’N and 42°48’N spanning over 1000 km from east to west, with a total area of 270, 000 km^2. The three main rivers of the Hexi Corridor, from west to east, are the Shule River, Heihe River and Shiyang River, originating from the Qilian Mountain. This region is one of the most important commodity grain bases in northwestern China due to its abundant land, light and heat resources (Fu et al., 2018) and shows typical features of arid zones, with annual mean precipitation of 50–150 mm and annual mean pan evaporation of 1500–2500 mm (Li et al., 2016). More than 60% of the crop planting area is occupied by cereal crops in the high-production counties such like Yongchang, Wuwei, etc. The main cereal crop types in the Hexi Corridor are spring wheat and spring corn, of which the growing season is during April to September. With the shortage of rainfall, water resources

scarcity is the limiting factor for regional prosperity and economic development in the Hexi Corridor.

3. Data and methods

3.1 Climatic data

Meteorological data, containing the historically observed daily precipitation, mean temperature, relative air humidity, were obtained from the China Meteorological Administration for 13 gauging stations within the Hexi Corridor over the period of 1970–2015. The monthly Bias Correction Spatial Disaggregation (BCSD) data from the Coupled Model Intercomparison Project Phase 5 (CMIP5) are utilized for the simulated historical and projected future data. The GCMs are downscaled by mainly two steps: (1) bias correction using a quantile mapping technique on a monthly and location-specific basis after regridded to a targeted resolution; (2) spatially translation of the biased GCMs to the targeted resolution(Wood et al., 2004). Four sets of GCMs (see Table 1) are chosen from the previously validated datasets that are suitable to simulate future precipitation and temperature variations in the Hexi Corridor (Zhang et al., 2015). However, the monthly projections of GCMs contain considerable uncertainties, especially for precipitation (Fu et al., 2013). Thus, the Linear Scaling (LS) method is employed for bias correction of both the precipitation and temperature outputs of the downscaled GCMs as follows:

$$P_{cor,m} = P_{raw,m} \times \frac{\mu(P_{obs,m})}{\mu(P_{\mathrm{raw},m})}, \tag{1}$$

$$T_{cor,m} = T_{raw,m} + \mu(T_{obs,m}) - \mu(T_{raw,m}), \tag{2}$$

where $P_{cor,m}$ and $T_{cor,m}$ are corrected precipitation and temperature of the mth month,

and $P_{raw,m}$ and $T_{raw,m}$ are the raw precipitation and temperature of the mth month. μ represents the mean value of precipitation and temperature of the given month m during the period 1970–2015.

3.2 Crop yield data

The original crop yield data of the period 1981–2012 were obtained from the China Economic and Social Development Statistical Database (http://tongji.cnki.net/kns55/index.aspx), Gansu Water Statistical Yearbook, collected by department of water management and agriculture. In statistical studies on the relationship between long-term crop yields and climatic factors, it is particularly important to separate trend yield and obtain accurate climatic yield. This is also vital to our study because the drought indices we utilized are calculated based on meteorological factors. The actual crop production is separated into three components (Niu et al., 2018; Fang et al, 2011) trend yield, climatic yield and the random error. The trend yield is the long-period output component that reflects the development level of productive forces in the historical period. Climatic yield is the component of the fluctuating part that is influenced by the short-term changing factors (mainly agricultural and meteorological disasters) dominated by climate variables. Trend yield is obtained by 5-yr moving average of the annual crop yield and climatic yield is calculated as the difference between actual yield and trend yield (random error is neglected).

3.3 Calculation of drought indices

The drought extent is described by drought indices in this study. We employ the

standardized precipitation evapotranspiration index (SPEI). Meanwhile, to assess the role that global warming plays in the drought evolution in the study area, the standardized precipitation index (SPI) is also calculated for comparison.

The calculation procedures of SPEI are as follows: (1) Potential evapotranspiration calculation (Thornthwaite, 1948):

$$PET = 16K(\frac{10T}{I})^m \tag{3}$$

where T is the monthly mean temperature; I is a heat index calculated by $I = 12(\frac{T}{5})^{1.514}$ and m is a coefficient depending on I: $m = 6.75\times10^{-7} I^3 - 7.71\times10^{-5} I^2 + 1.79\times10^{-2} I + 0.492$ and K is a correction coefficient calculated as a function of the latitude and month. (2) A simple measure of water surplus for the analyzed month:

$$D_j = P_j - PET_j \tag{4}$$

The calculated D_j values are aggregated at different time scales. The difference $D_{i,j}^k$ in a given month j and year i depends on the chosen time scale k. For example, the accumulated difference for one month in a particular year i with a 12-month time scale is calculated using:

$$X_{i,j}^k = \sum_{l=13-k+j}^{12} D_{i-1,l} + \sum_{l=1}^{j} D_{i,l} \text{ , if } j < k \tag{5}$$

$$X_{i,j}^k = \sum_{l=j-k+1}^{j} D_{i,l} \text{ , if } j \geq k \tag{6}$$

where $D_{i,l}$ is the *P-PET* difference in the first month of the year i. (3) Normalize the water balance to obtain the SPEI index series: A three-parameter log-logistic

distribution is used, with the probability density function expressed as:

$$f(x) = \frac{\beta}{\alpha}\left(\frac{x-\gamma}{\alpha}\right)^{\beta-1}\left[1+\left(\frac{x-\gamma}{\alpha}\right)^{\beta}\right]^{-2} \quad (7)$$

where α , β , and γ are scale, shape, and origin parameters, respectively, for D values in the range $(\gamma > D)$.

The probability distribution function of the D series is given by:

$$F(x) = \left[1+\left(\frac{\alpha}{x-\gamma}\right)^{\beta}\right]^{-1} \quad (8)$$

with $F(x)$ the SPEI can easily be obtained as the standardized values of $F(x)$:

$$SPEI = W - \frac{C_0 + C_1 W + C_2 W^2}{1 + d_1 W + d_2 W^2 + d_3 W^3} \quad (9)$$

where $W = \sqrt{-2\ln(P)}$ for $p \le 0.5$ and P is the probability of exceeding a determined D value, $P = 1 - F(x)$. If $P > 0.5$, then P is replaced by $1 - P$ and the sign of the resultant SPEI is reversed. The constants are $C_0 = 2.515517$, $C_1 = 0.802853$, $C_2 = 0.010328$, $d_1 = 1.432788$, $d_2 = 0.189269$, and $d_3 = 0.001308$.

The process of SPI calculation can be summarized into the following steps: (1) Choose the aggregation temporal scale, denoted by k and the monthly precipitation is aggregated to the time scale k with the same procedure as D_j in SPEI. (2) A gamma probability density function (PDF) is performed separately for each month. The PDF g(x) and the cumulative distribution function G(x) are listed below:

$$g(x) = \frac{1}{\beta^{\alpha}\Gamma(\alpha)} x^{\alpha-1} e^{-x/\beta}, \quad \text{for } x > 0 \quad (10)$$

$$G(x) = \frac{1}{\beta^{\alpha}\Gamma(\alpha)} \int_0^x t^{\alpha-1} e^{-t/\beta} dt, \quad \text{for } x > 0 \quad (11)$$

$$H(x) = q + (1-q)G(x) \quad (12)$$

where α, β are shape and scale parameters estimated by the maximum likelihood method and x is the cumulative precipitation amount in Eq. (10). Since precipitation is not continuous over time, Eq. (13) is utilized where q is the probability of zero. (3) Following the approximate conversion provided by Abramowitz and Stegun (1965), SPI is obtained by:

$$SPI = -(t - \frac{c_0 + c_1 t + c_2 t^2}{1 + d_1 t + d_2 t^2 + d_3 t^3}), \quad t = \sqrt{\ln(\frac{1}{H(x)^2})} \quad \text{for } 0 < H(x) < 0.5 \tag{13}$$

$$SPI = (t - \frac{c_0 + c_1 t + c_2 t^2}{1 + d_1 t + d_2 t^2 + d_3 t^3}), \quad t = \sqrt{\ln(\frac{1}{(1 - H(x))^2})} \quad \text{for } 0.5 < H(x) < 1.0 \tag{14}$$

with $c_0 = 2.515517$, $c_1 = 0.802853$, $c_2 = 0.010328$, $d_1 = 1.432788$, $d_2 = 0.189269$, and $d_3 = 0.001308$.

As for the calculation of potential evapotranspiration (PET), most of the studies utilized the Thornthwaite (PET_th) or the Penman-Monteith (PET_pm) methods (Thornthwaite, 1948; Burke et al., 2006; Shuttleworth, 1992). We adopt the Thornthwaite method, considering that the GCMs only provide precipitation and temperature information and we want to make the PET results consistent and comparable in both historical and future time horizons. In addition, previous studies (e.g., Ke and Wang, 2013) have shown that the differences of PET_th and PET_pm are small in northwestern China and the trends of the regional averaged PET_th and PET_pm are similar in the past decades. Trend analysis of climatic factors and drought indices utilizes the Mann-Kendall method (Mann, 1945; Kendall, 1975).

3.4 Correlation between climatic yield and drought index

Correlation analysis is commonly used when revealing the relationship between

two variables (Ichii et al., 2002). Correlation between drought indices and decomposed crop yields are assessed using the Pearson correlation coefficient, which is calculated as follows:

$$r_{X,Y} = \frac{\sum(\mathrm{X}-\overline{X})(\mathrm{Y}-\overline{Y})}{\sqrt{\sum(\mathrm{X}-\overline{X})^2\sum(\mathrm{Y}-\overline{Y})^2}} \quad (15)$$

where X and Y are the time series of two variables, $\overline{X}$ and $\overline{Y}$ are the mean values of the two series. The correlation coefficient $r_{X,Y}$ ranges from –1 to +1, with –1 indicating that the two variables are perfectly negatively correlated and +1 indicating a perfect positive correlation. In this study, the correlation was computed between the time series of crop yield and 1, 3, 12-month drought indices (SPI and SPEI).

4. Results and discussion

4.1 Changes of meteorological factors and drought severity in recent decades

Annual rainfall in the Hexi Corridor is about 130 mm, which is far below the average situation of other agricultural regions in China, especially the eastern and southern parts of China. The average rainfall during the period of 1970–2005 is 122 mm year^{-1}, but the value has risen to 142 mm year^{-1} during 2006–2015, which indicates that the annual precipitation has increased by about 16% in the last decade. An turning point can be observed around the year 2000 (Fig. 2(b)) that moving average value of mean temperature exceeded the average of the year 1970–2015. The average of T_{mean} in the Hexi Corridor is 7.2℃ before 2000 and 8.4℃ after 2000, which increased by 1.2℃ during the study period.

It is considered that the wetness/dryness trend is mainly determined by the water

balance in a region. The anomaly of temperature results in the consistent increase of potential evapotranspiration (PET): a significant shift around year 1997 and stays at a high level in the recent two decades. The relative air humidity has been fluctuating between 44%–51% during the period 1970–2010 and shows a significant drop from year 2010, among which the value is below 41% in 2013. This may become an indicator of the drought situation in the recent years in the Hexi Corridor.

Figure 3 shows the temporal evolutions of regional averaged SPEI and SPI with different time scales (1, 3, and 12-month). Shorter time scale drought indices can detect more drought events for that taking consider into only the current month (1-month scale) and the previous 2 months (3-month scale), their responses to the change of climatic variables are more instant. But to investigate the long-term changing pattern of drought condition, a longer time scale is more appropriate and have a more intuitive presentation of the trend. In the early stage of the 12-month drought evolution (see Fig. 3(c)), drought condition indicated by SPI is severer than that of SPEI, which is because precipitation anomaly is more significant than that of temperature over that period. In the middle stage, the variations of the two indices are almost consistent. However, continuous drought in the recent years is displayed by SPEI as a result of the significant increase of temperature while SPI exhibits an improved situation of drought events because of the positive precipitation anomaly. Given that the variation of PET is larger than that of the rainfall over the study period, we consider that in the arid regions like the Hexi Corridor where evaporation is large, SPEI is more appropriate than SPI to characterize drought features.

Spatial distribution of trends for SPEI and SPI over the historical stage is shown in Figure 4. The southeast of the corridor, which is occupied by some important crop production districts such as Minqin, Yongchang and Wuwei counties, shows upward trends both indicated by SPI and SPEI during the period of 1970–2015 (Fig 4), which may be conductive to crop growth in these districts. A large proportion of the region shows significant wet trend showed by the two indices in the last decades, which is correspondent to the finding of some previous studies that also point out the significant trends toward wet conditions were mainly observed in the northwestern part of China (Shi et al., 2003; Tao et al., 2014; Zhai et al., 2014). The performances of SPEI and SPI are different in terms of describing drought condition spatially. The difference between the two indices is small in the relatively humid area of the study region (i.e., the southeast part), but in the northwest part, where the environment is more arid, SPEI and SPI show large difference or even the opposite result in the county Anxi.

4.2 Response of crop production to meteorological droughts in the Hexi Corridor

Correlation coefficients between climatic crop production and drought indices for the crop growing season are studied during the period 1985–2012 (Fig. 7). It is evident that correlation between SPEI and crop yields is higher than that of SPI for all the months during April to September, which reveals that drought caused by evaporation anomaly is the most possible reason for the loss of crop production in the Hexi Corridor. The changing patterns of correlation coefficients are unimodal curves with the correlation increasing first and then decreasing as time scale gets larger. It is

observed from Figure 5, 3-month scale growing season SPEI is most related to crop growth, which indicates that crop growth is most influenced by seasonal drought condition and in addition, the correlation of SPEI value for the month July is highest among the 3-month SPEI (named as SPEI3-7 below). This is reasonable because the calculation of SPEI3-7 utilizes climatic variables in May, June and July when cereal crops are during the seedling, jointing and anthesis period, which is proved by field experiments that water deficit during these periods has the greatest impact on crop yield of corn in Northwestern China (Wang et al., 2019). Different from the study of correlation between rice yield and drought which finds that crop yield is most related to 1-month SPEI (Prabnakorn et al., 2018), rice grown in Thailand is rainfed while crops in the Hexi Corridor rely greatly on irrigation regime, situation of crop does not change immediately with climatic changes.

In order to apply this correlation to regional management, we also analyze the correlation between regional SPEI values with regional climatic yields (Fig 6). In the northwest part of the study area (county Subei, Dunhuang, etc), the correlation is low and even negative, which is due to the topography: those areas are mainly alpine or desert where crops are seldom planted, however, the SPEI value is station-based while the crop yield is officially recorded in a county level, so datasets are not matched enough to reflect the real relationship between drought and crop yield. The highly correlated areas are mainly distributed in the agricultural developed area in the east part of the corridor such like Yongchang, Shandan, Wuwei and Minqin (named as D1-D4 in Figure 6), etc. Though the county Anxi, Tianzhu and Yumen also show high

correlations between SPEI and climatic yield, they excluded in the analysis for that the crop planting area is too small compared to the total land area, and the topography is mountainous area and desert, making it incomparable with other places that are located in the oasis and plain. Thus, a preliminary conclusion can be drawn that extreme events significantly influence crop production in the Hexi Corridor.

The objective of the investigation of relationship between drought indices and climatic crop yield is to identify the pattern of yield change with drought condition variation caused by climatic change, which is also helpful to reveal the ecological vulnerability of cultivated lands in the high-crop-yield districts (i.e., D1-D4). The results of linear regression of the 3-month SPEI value for July (SPEI3-7) and climatic yield of different districts are shown in Figure 7. Climatic yield increases as the drought condition detected by SPEI3-7 gets wetter, which means that yield loss gets larger as drought becomes severer. The intersections of each regression line and the X-axis are the critical points (i.e. defined as SPEIc=-intercept/slope) indicating the impact of the climate-induced drought on annual crop yield, beyond which climate is beneficial to crop growth of the year. This critical point, $SPEI_c$, represents the different extent of vulnerability of the studied district and the drought resistance ability of the cereal crops in that district. As the figure shows, $SPEI_c$ is different for different area. For example, climate will do harm to annual crop yield of the county Yongchang (D1) when SPEI reaches -0.77 while crop yield will be negatively affected after SPEI reaches around -1.35/-1.27 for Shandan and Minqin and -1.02 for the county Wuwei, indicating that crops in Shandan and Minqin have better drought

resistance or the water management activities like irrigation is more effective there. The impact of drought do not perform equally through all growth stages and regions (Geng et al., 2016; Peña - Gallardo et al., 2018), because it is proved that local climatology and water availability are also important in the responding pattern of crop yield to drought (Peña-Gallardo et al., 2019). Thus, though the changing patterns are similar among the four districts, $SPEI_c$ value is unequally distributed across the region as a result of different planting structure, crop types and water managing strategies.

4.3 Projections of climate change and drought indices in the future

Possible changes of projected precipitation and mean temperature during the period 2017–2050 by different GCMs are displayed in Figure 8. For precipitation, RCP4.5 emission scenario in the RCP2.6 and RCP4.5 emission scenarios, slightly decreases were observed during year 2034–2050 compared to the period 2017–2033. But precipitation for RCP8.5 increased in the latter time period. Temperature for all the three emission scenarios show a significant increase in the period of 2034–2050. This can also be revealed by the evolution of drought indices for the future period (Figure 9). Potential evapotranspiration shows the similar trend to the variation of temperature. In the former time period, the variation ranges of PET are between 2~12% for different RCP scenarios, and in the latter period, the trend expands to 12~23%, among which the RCP8.5 scenario shows the most significant increase.

A significant downward trend over the period 2030–2050 is illustrated by SPEI, indicating that temperature anomaly is significant and difference between the three emission scenarios is small, among which RCP2.6 demonstrates the most serious

drought condition during the period. The pattern of drought frequency change is also different between SPEI and SPI but consistent across RCPs. For SPEI, drought events will occur more frequently in the latter time stage as indicated by all the three emission scenarios and drought frequency change between the two future stages is largest for the RCP2.6 scenario. What can be seen by combining the two figures of SPEI is that climate change in the future will make drought more frequent, but less severe across the region. For SPI, there is a fluctuation around 0 over the study period by all the scenarios, but drought frequency decreases in the latter period of the two future stages. Fig. 10 shows the change of SPEI and SPI between 2017-2033 and 2034-2050 in the Hexi Corridor. It is evident that values of SPEI decrease in all the 13 sites, among which the differences are larger than -1 in 5 stations. But in contrast, the differences between the two future stages are all positive values for SPI, showing that the condition is wetter in the future decades. Overall, the two drought indices behave more differently when the temperature variation becomes larger both temporally and spatially, which can be attributed to the role of changes in PET. Thus, it can be concluded that as global warming becomes severer in the future, the role of evapotranspiration cannot be ignored anymore in the studies of drought monitoring for the region.

We can identify future drought events after obtaining the future drought evolution and the critical points ($SPEI_c$ value, the red dash lines in Figure 11), we can predict future drought events that have negative impact on crop yield for different emission scenarios after obtaining the SPEI value of different districts. Figure 11

shows the SPEI variation of the four districts selected for RCP2.6, RCP4.5 and RCP8.5. In general, SPEI calculated by RCP4.5 detects the smallest amount of drought events for the four districts compared to the other two scenarios. Overall, the studied districts are still exposed to high risk of crop production loss. Though the cereal crops in the Hexi Corridor are resistant to drought to some extent, adaptative and crop management measures need to be seriously planned especially in the period of 2040s–2050s to avoid food disasters in the future.

5. Conclusion

Historical and future trends of meteorological data from 13 weather stations and 4 GCMs over the Hexi Corridor and the period 1970–2050 were investigated. A continuous increasing trend was detected in the variation of temperature, which is a vital signal for the potential warming effect and aggravated drought condition over the study region. As a result, drought illustrated by SPEI shows a significant downward trend. By analyzing the relationship between SPEI and the decomposed climatic yield, the critical points of the SPEI-production curves, which might be used to forecast future food disasters, can be identified for the important food producing areas. Different SPEI value for each critical point are reflections of the ecological vulnerabilities of different districts. And 2040s and 2050s are found to be most exposed to food disaster for D1-4 in the three future decades, which can perform as references for future water management for this region.

Drought indices have been widely used in drought monitoring worldwide due to its easy access and this study reveals the fact that drought index considering water

demand (evapotranspiration) has better performance in monitoring drought condition and higher correlation with crop growth in arid and semiarid regions like the Hexi Corridor, which is consistent with the findings of Mkhabela et al (2010). Thus, compared to SPI that focuses only on water supply (precipitation), SPEI is more appropriate to be utilized in analyzing the impact of drought on crop yield.

As indicated by the drought indices, though precipitation and temperature have both been increasing in the late 20th century and early 21st century over the Hexi Corridor, recorded as a trend toward warm and wet by some previous studies, the drought condition detected by SPEI is getting severer considering water balance in the area. There is still a high risk of severer drought conditions in the future and policies should be made to avoid big crop losses such like introducing more drought-tolerant varieties and further improving water use efficiency in the water scarce districts. However, there still exists various data-related and methodological challenges to be addressed for an accurate estimation of drought impacts on crop productivity (Siebert et al., 2017). Though errors exist in different steps of this study and it is necessary to perform some further analysis in the study of drought-production relations by employing more accurate datasets and more robust research methods, the information provided in this research is still valuable in guiding the agricultural management in arid and semiarid areas in China and is a good reference when taking adaptive measures in the face of climate change.

Acknowledgements

This work was financially supported by the National Key Research and Development

Plan (2016YFC0400207), the National Natural Science Foundation of China (51679233), and the Program of Introducing Talents of Discipline to Universities (B14002). The authors thank the two anonymous reviewers for the valuable comments and suggestions on an earlier version of the paper, which resulted in a more complete and accurate presentation of the work performed.

References

Abramowitz, M., Stegun, A., 1965. Handbook of Mathematical Functions: with Formulas, Graphs and Mathematical Tables. Dover Publications Inc., New York.

Arshad, S., Morid, S., Mobasheri, M.R., Alikhani, M.A., Arshad, S., 2013. Monitoring and forecasting drought impact on dryland farming areas. Int. J. Climatol. 33, 2068-2081.

Bruins, H.J., Berliner, P.R., 1998. Bioclimatic aridity, Climatic Variability, Drought and Desertification: Definition and Management Options. The Arid Frontier. Springer, pp, 97-116.

Burke, E.J., Brown, S.J., Christidis, N.,2006. Modeling the recent evolution of global drought and projections for the twenty-first century with the Harley Centre climate model. J. Hydrometeor. 7,1113-1125.

Dai, A., 2011. Drought under global warming: a review. WIREs Climate Change 2, 45–65.

Fang, S.B., 2011. Exploration of method for discrimination between trend crop yield and climatic fluctuant yield. J. Nat. Disasters 20 (6), 13–18.

Fu, G.B., Liu, Z.F., Charles, S.P., Xu, Z.X., Yao, Z.J., 2013. A score-based method for assessing the performance of GCMs: A case study of southeastern Australia. J. Geophys. Res. Atoms. 118, 4154-4167.

Fu, J., Niu, J., Sivakumar, B., 2018. Prediction of vegetation anomalies over an inland river basin in north-western China. Hydro. Processes. 32, 1814-1827.

Geng, G., Wu, J., Wang, Q., Lei, T., He, B., Li, X., Mo, X., Luo, H., Zhou, H. and Liu, D, 2016. Agricultural drought hazard analysis during 1980–2008: a global perspective. Int. J. of Climat. 36, 389–399.

Guttman, N.B., 1998. Comparing the Palmer Drought Index and the Standardized Precipitation Index. J. Amer. Water Resour. Assoc. 34, 113-121.

Ichii, K., Kawabata, A., Yamaguchi, Y., 2002. Global correlation analysis for NDVI and climatic variables and NDVI trends: 1982-1990. Int. J. Remote Sens. 23, 3873-3878.

Ke, W., Wang, L., 2013. Reexamination of the Aridity Conditions in Arid Northwestern China for the last decade. J. Climate. 26, 9594-9602.

Kendall, M.G., 1975. Rank Correlation Measures, Charles Griffin, London, UK.

Kola, P., Trnka, M., Brazdil, R., Hlavinka, P., 2014. Influence of climatic factors on the low yields of spring barley and winter wheat in Southern Moravia (Czech Republic) during the 1961-2007 period. Theor. Appl. Climatol. 117, 707–721.

Lesk, C., Rowhani, P., Ramankutty, N., 2016. Influence of extreme weather disasters on global crop production. Nature. 529, 84-87.

Li, X.L., Zhang, X.T., Niu, J., Tong, L., Kang, S.Z., Du, T.S., Li, S.E., Ding, R.S., 2016. Irrigation water productivity is more influenced by agronomic practice factors than by climatic factors in Hexi Corridor, Northwest China. Sci. Rep. 6, 37971.

Liu Ming, Li Suju, Wu Jianjun, He Haixia, Huang He, Lü Aifeng, 2015. Change of drought and its impact on potential yield of wheat in agricultural region of Shan-Gan-Ning region in 1961-2010. Transactions of the Chinese Society of Agricultural Engineering (Transactions of the CSAE), 31(18), 147-154. (in Chinese with English abstract)

Lobell, D.B., Bänziger, M., Magorokosho, C., Vivek, B., 2011. Nonlinear heat effects on African maize as evidenced by historical yield trials. Nat. Clim. Chang. 1, 42–45.

Mann, H.B., 1945. Nonparametric tests against trend. Econometrica 13, 245–259.

Mckee, T.B., N.J. Doesken, J. Kleist., 1993. The relationship of drought frequency and duration to time scales. Prepints, Eighth Conf. on Applied Climatology. Anaheim, CA, Amer. Meteor. Soc. 179-184.

Mishra, A.K., Singh, V.P., 2011. Drought modelling – a review. J. Hydrol. 4031, 157-175.

Mkhabela, M., Bullock, P., Gervais, P., Finlay, G., Sapirstein, H., 2010. Assessing indicators of agricultural drought impacts on spring wheat yield and quality on the Canadian prairies. Agr Forest Meteoro. 150, 399-410.

Niu, J., Chen, J., 2014. Terrestrial hydrological responses to precipitation variability in Southwest China with emphasis on drought. Hydrological Sciences Journal 59(2), 325-335.

Niu, J., Chen, J., Sun, L., 2015. Exploration of drought evolution using numerical simulations over the Xijiang (West River) basin in South China. J. Hydrol. 526, 68–77.

Niu, J., Kang, S.Z., Zhang, X.T., Fu, J., 2017. Vunlnerability analysis based on drought and vegetation dynamics. Ecological Indicators, doi : 10.1016/j.ecolind.2017.10.048

Niu, J., Liu, Q., Kang, S.Z., Zhang, X.T., 2018. The response of crop water productivity to climatic variation in the upper-middle reaches of the Heihe River basin, Northwest China. J. Hydrol. 563, 909-926.

Palmer, W.C., Meteorological drought. US Department of Commerce. Weather Bureau, Research Paper No. 45, 58 pp.

Peña-Gallardo, M., Vicente-Serrano, S.M., Quiring, S., Svoboda, M., Beguería, S. and Hannaford, J, 2018. Effectiveness of drought indices in identifying impacts on major crops across the USA. Climate Research, 75, 221–240.

Peña-Gallardo, M., Vicente-Serrano, S.M., Quiring, S., Svoboda, M., Hannaford, J.,

Tomas-Burguera, M., et al., 2019. Response of crop yield to different time-scales of drought in the United States: Spatio-temporal patterns and climatic and environmental drivers. Agr Forest Meteoro. 264, 40-55.

Poptop, V., Turkott, L., Koznarova, V., Mozny, M., 2010. Drought episodes in the Czech Republic and their potential effects in agriculture. Theor. Appl. Climatol. 99, 373-388.

Poptop, V., Mozny, M., Soukup, J., 2012. Drought evolution at various time scales in the lowland regions and their impact on vegetable crops in the Czech Republic. Agr Forest Meteoro. 156, 121-133.

Prabnakorn, S., Maskey, S., Suryadi, F.X., de Fraiture, C., 2018. Rice yield in response to climate trends and drought index in the Mun River Basin, Thailand. Sci. Total. Env. 621, 108-119.

Qin, D.H., Zhang, J.Y., Shan, C.C et al., 2015. China national assessment report on risk management and adaptation of climate extremes and disasters. Science Press, Beijing, pp, 70-124.

Quiring, S.M., Papakryiakou, T.N., 2003. An evaluation of agricultural drought indices for the Canadian prairies. Agr Forest Meteorol. 118, 49-62.

Richard, R., Heim, J.R., 2002. A review of twentieth-century drought indices used in the United States. Bulletin of the American Meteorological Society. 83, 1149-1165.

Shen, C., Wang, W.C., Hao, Z., Gong, W., 2007. Exceptional drought events over eastern China during the last five centuries. Climatic Change. 85, 453-471.

Shi, Y.F., Shen, Y.P., Li, D.L. et al., 2003. Discussion on the present climate change from warm-dry to warm-wet in Northwest China. Quat Sci. 23, 152-164.

Shuttleworth, W.J., 1992. Evaporation. Handbook of Hydrology, D.R., Maidment, Ed.,

McGraw-Hill, 4.4-4.53.

Siebert, S., Webber, H., Rezaei, E.E., 2017. Weather impacts on crop yields - searching for simple answers to a complex problem. Environ. Res. Lett. 12, 81001.

Sivakumar, B., 2011. Global climate change and its impacts on water resources planning and management: assessment and challenges. Stochastic Environment Research and Risk Assessment 25, 583–600.

Tack, J., Barkley, A., Nalley, L.L., 2015. Effect of warming temperatures on U.S. Wheat yields. Proc. Natl. Acad. Sci. 112 (22), 6931–6936.

Tao, H., Borth, H., Fraedrich, K., Su, B.D., Zhu, X.H., 2014. Drought and wetness variability in the Tarim River basin and connection to large-scale atmosphere circulation. Int J Climatol. 34, 2678-2684.

Thornthwaite, C.W., 1948. An approach toward a rational classification of climate. Geogr. Rev. 39,55-94.

Vicente-Serrano, S.M., Beguería, Santiago, López-Moreno, Juan I., 2010. A Multi-scalar drought index sensitive to global warming: the Standardized Precipitation Evapotranspiration Index – SPEI. J. Clim. 23, 1696–1718.

Vicente-Serrano, S.M., Beguería, Santiago, Lorenzo-Lacruz, Jorge, Camarero, Jesús Julio, López-Moreno, Juan I., Azorin-Molina, Cesar, Revuelto, Jesús, Morán-Tejeda, Enrique, Sánchez-Lorenzo, Arturo, 2012. Performance of drought índices for ecological, agricultural and hydrological applications. Earth Interact. 16, 1–27.

Wang, H., Vicente-Serrano, S.M., Tao, F., Zhang, X., Wang, P., Zhang, C., Chen, Y., Zhu, D., Kenawy, A.E., 2016a. Monitoring winter wheat drought threat in Northern China using

multiple climate-based drought indices and soil moisture during 2000-2013. Agric. For. Meteorol. 228–229.

Wang, J.T., Kang, S.Z., Du, T.S., Tong, L., Ding, R.S., Li, S.E., 2019. Estimating the upper and lower limits of Kernel weight under different water regimes in hybrid maize seed production. Agric. Water Manag. 213, 128-134.

Wang, Q., Wu, J., Li, X., Zhou, H., Yang, J., Geng, G., An, X., Liu, L., Tang, Z., 2016b. A comprehensively quantitative method of evaluating the impact of drought on crop yield using daily multi-scale SPEI and crop growth process model. Int. J. Biometeorol. 1–15

Wilhite, D.A., Glantz, M.H., 1985. Understanding: the drought phenomenon: the role of definitions. Water Int. 10 (3), 111-120.

Wood, A.W., Leung, L.R., Sridhar, V., Lettenmaier, D.P., 2004. Hydrologic implications of dynamical and statistical approaches to downscaling climate model outputs. Climatic Change. 15 (62), 189-216.

Yihdego, Y., Vaheddoost, B., AL-Weshah, R.A., 2019. Drought indices and indicators revisited. Arabian J. Geosci. 12, 69.

Zhai J.Q., Gao, B., Zhu, X.Y., 2014. Fact sheet on climate disaster in China. In: Wang, G.W., Zheng, G.G. (eds) Annual report on actions to address climate change. Social Sciences Academic Press, Beijing.

Zhang, Y.Y., Fu, G.B., Sun, B.Y., Zhang, S.F., Men, B.H., 2015. Simulation and classification of the impacts of projected climate change on flow regimes in the arid Hexi Corridor of Northwest China. J. Geophs. Res. Atmos. 120, 7429-7453.

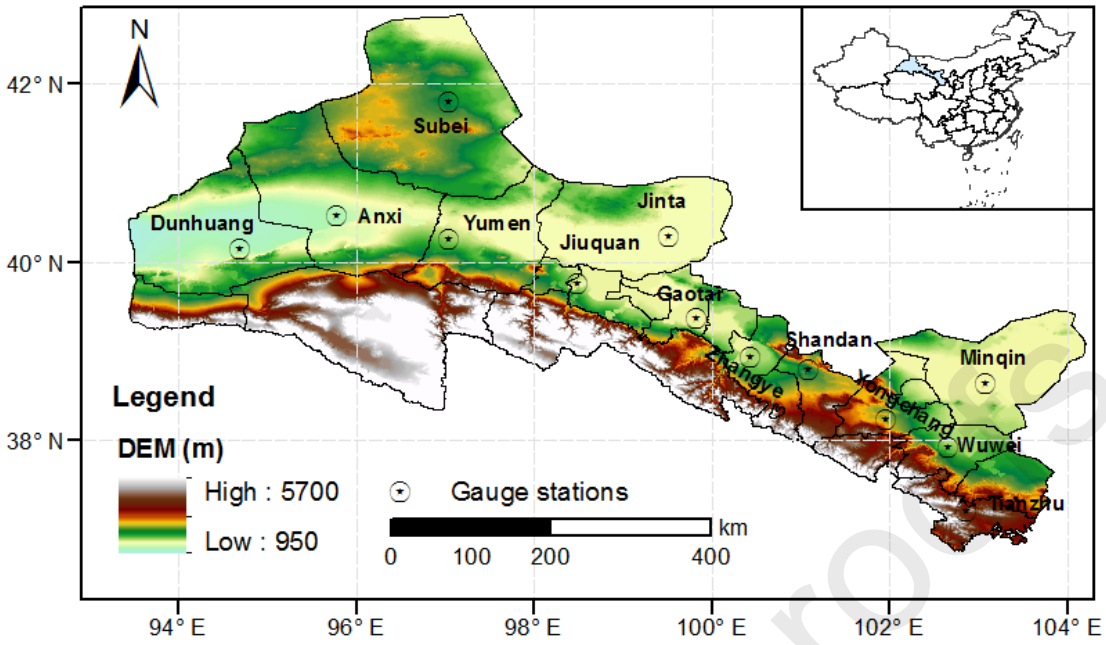

Fig. 1 Location of Hexi Corridor and the spatial distribution of the weather stations.

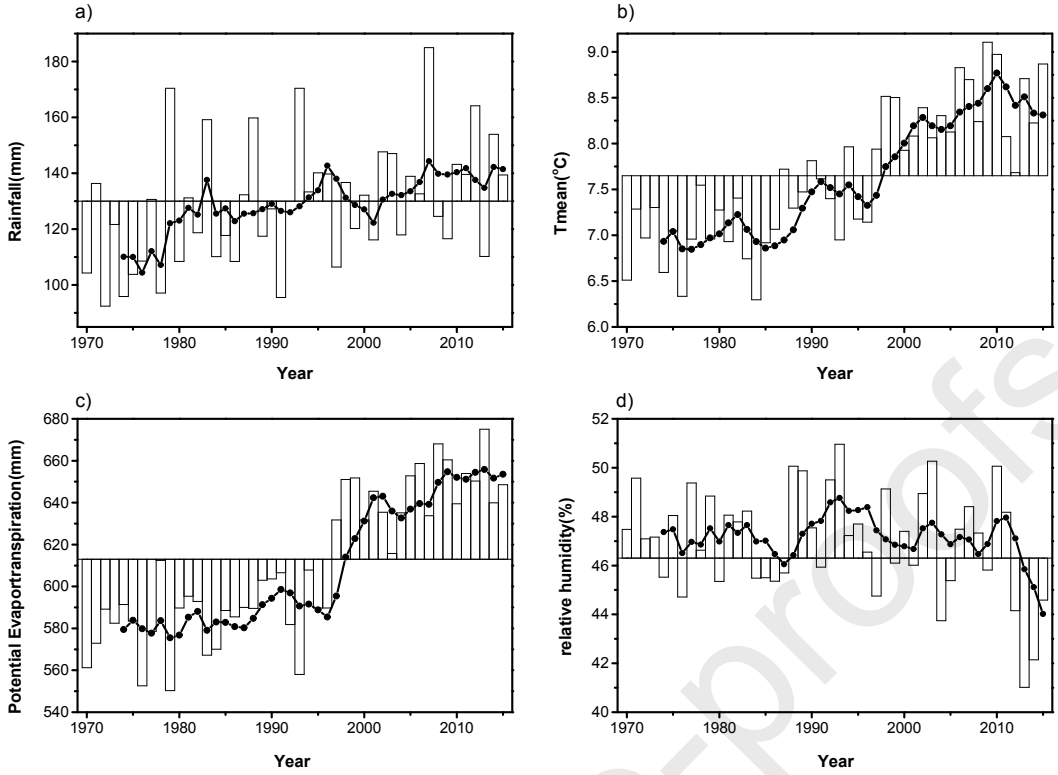

Fig. 2 Time series of the annual mean of (a) precipitation, (b) air temperature, (c) potential evapotranspiration, and (d) air relative humidity. All bars above are averaged for the 13 weather stations in the Hexi Corridor; the curves indicate the 5-yr running average values.

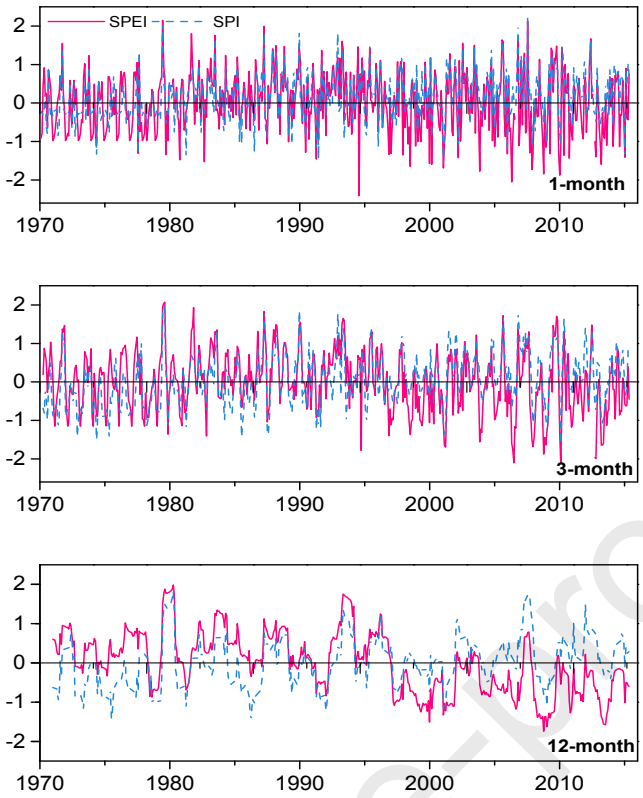

Fig. 3 Multi-scale (1-, 3-, and 12-month) evolutions of SPEI and SPI time series during the period 1970-2015.

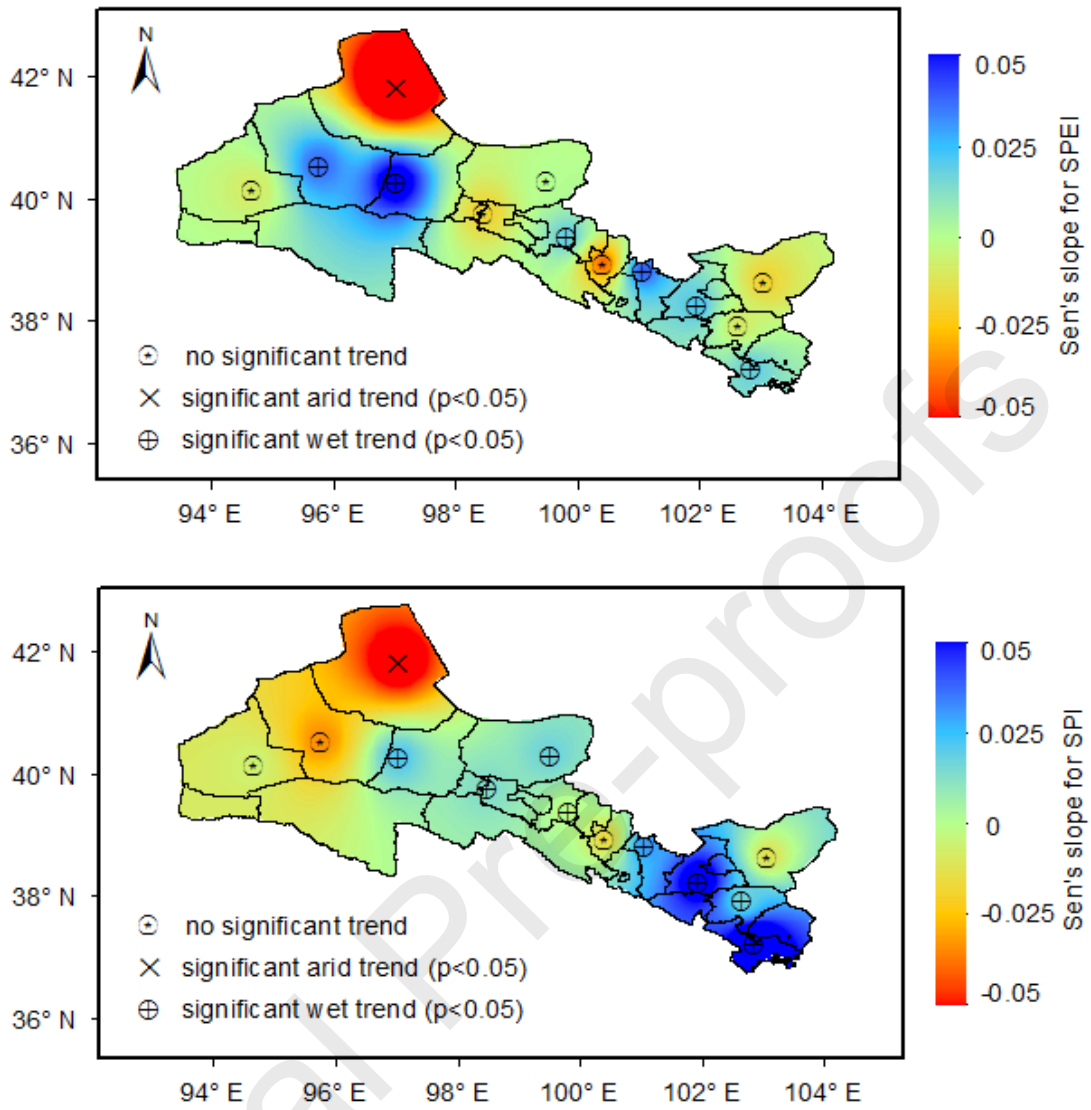

Fig. 4 Mann-Kendall test results for 12-month SPEI (upper panel) and SPI (lower panel) time series for the period 1970–2015 in the Hexi corridor.

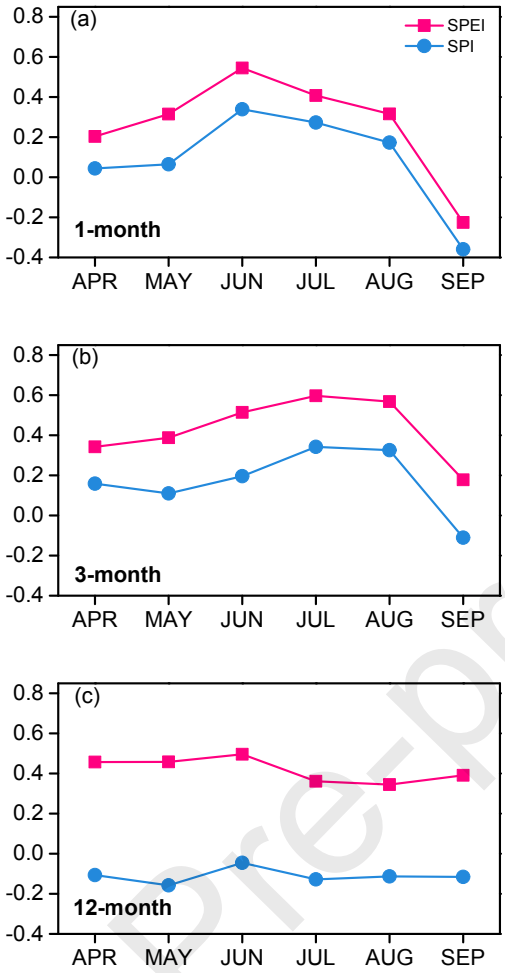

Fig. 5 Multiscale-correlation between climatic yield and drought indices of different months in the growing season under different time scales (1-, 3-, and 12-month).

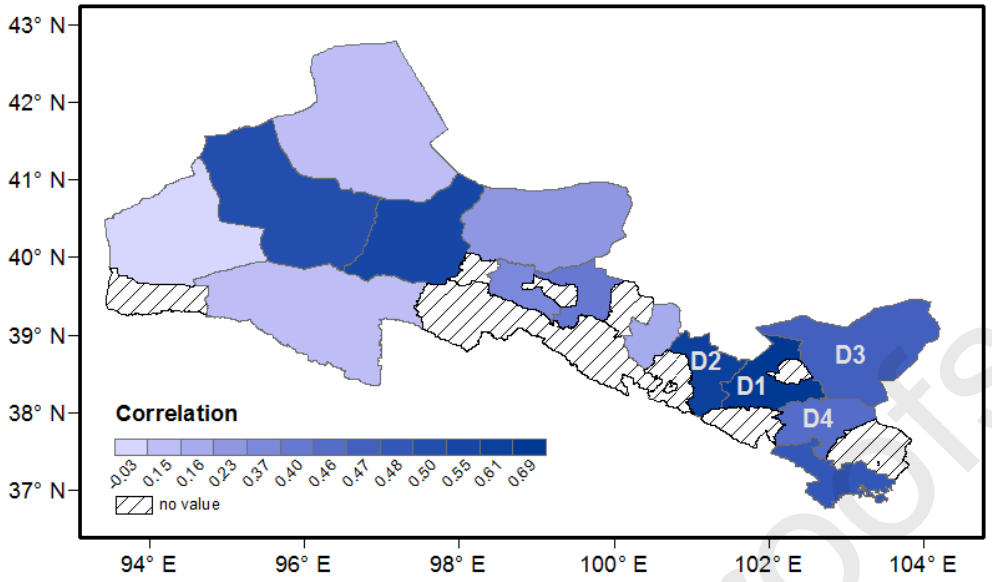

Fig. 6 spatial distribution of correlation between climatic yield and SPEI3-7 (the 3-month SPEI value for July) in different districts in the Hexi Corridor.

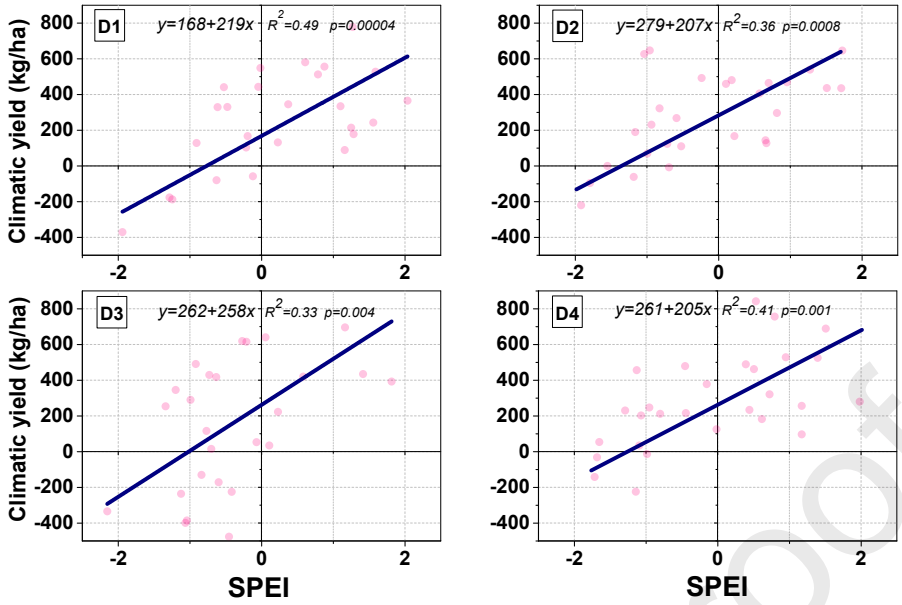

Fig. 7 Scatter plot for crop yield variability against the 12-month SPEI values. Blue lines represent linear regression of the two variables. D1-D4 are the four crop production districts in the Hexi Corridor: Yongchang, Shandan, Wuwei, Minqin.

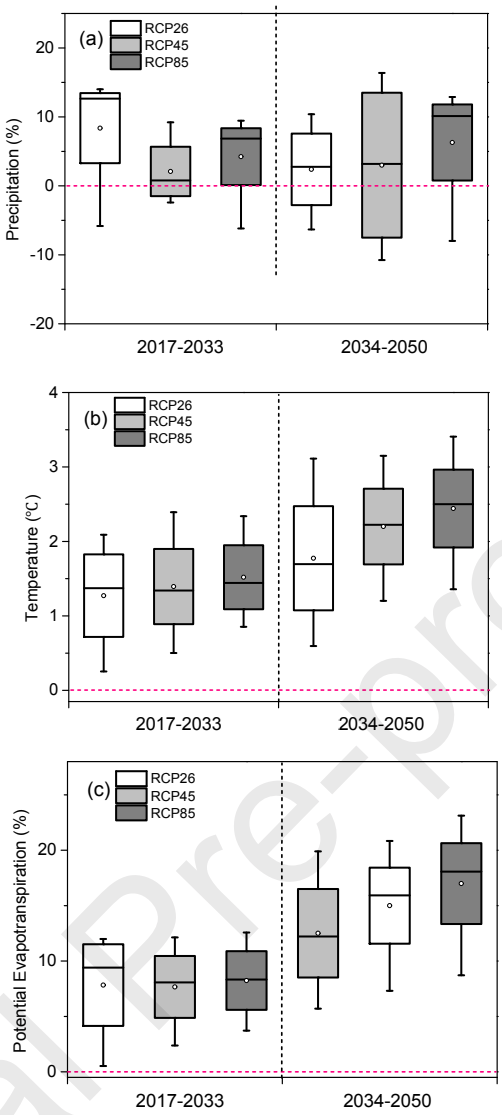

Fig. 8 The variations of (a) precipitation; (b) mean temperature in the two future stages (2017-2033 and 2034-2050). The variation is the difference between each future stage and the historical period for every GCM. Each box plot illustrates the 25th, 50th, and 75th percentile values, and the vertical bars define the 10th and 90th percentile values. The red dash line represents no difference (0) between the baseline and future periods.

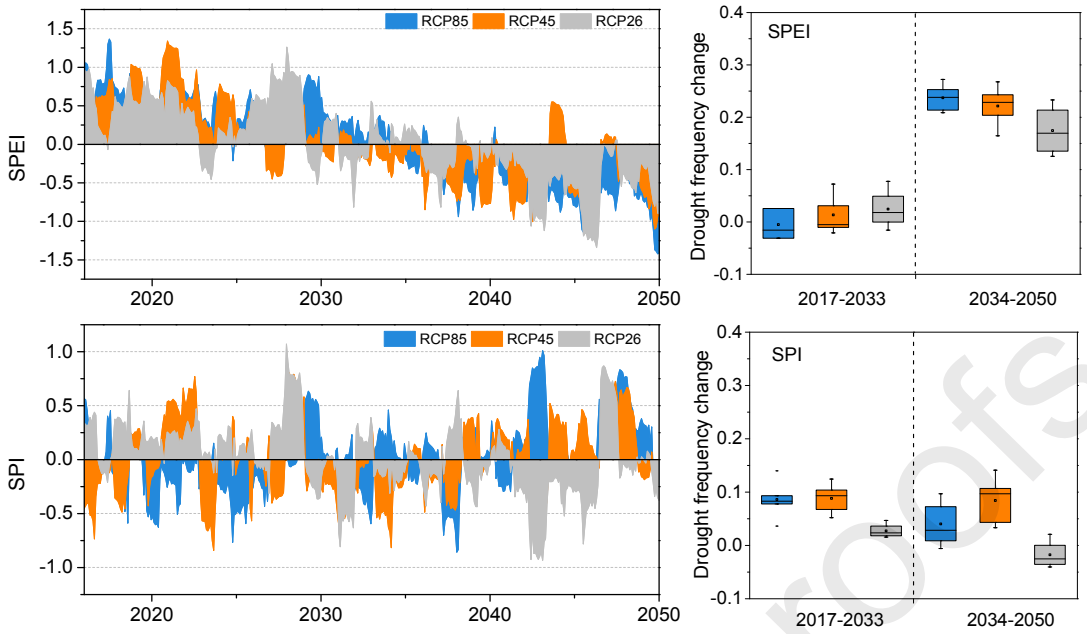

Figure 9: 12-month SPEI and SPI evolution under different future emission scenarios (left panel) and drought frequency (proportion of years when drought indices are negative) changes between two future stages and observed values (baseline: 2000-2015). The drought indices are averaged among all the GCMs for the three emission scenarios.

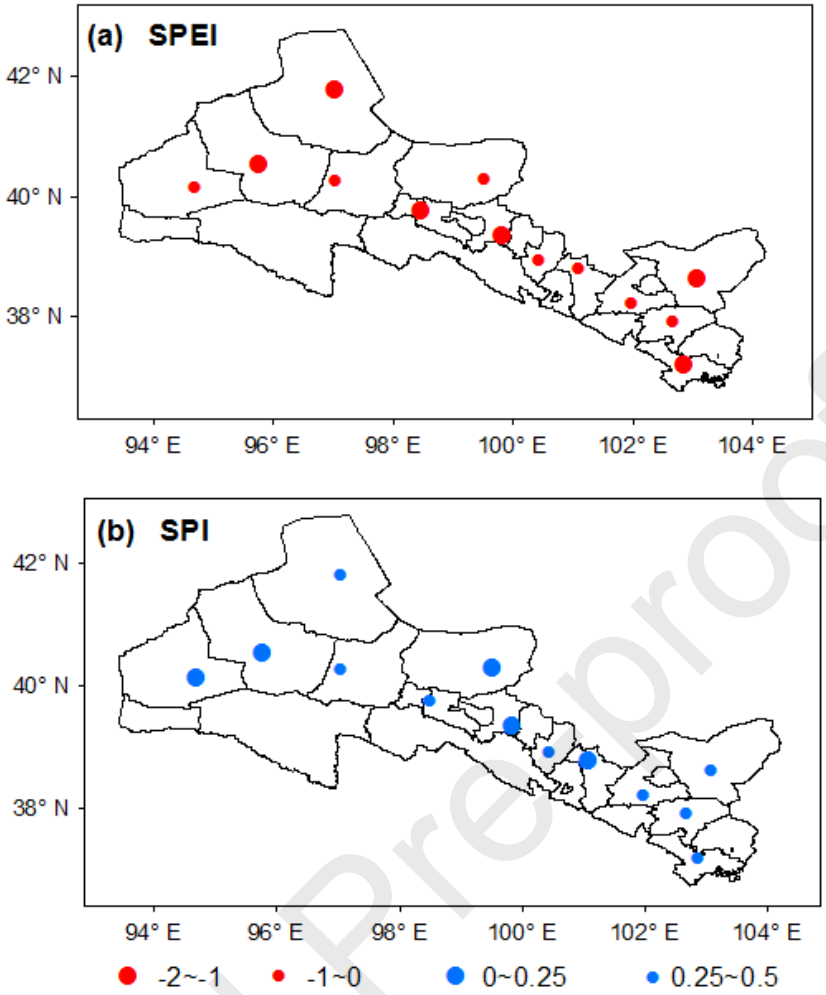

Fig. 10 spatial distribution of the change of drought indices of two future stages (2034-2050 minus 2017-2033) over the Hexi Corridor.

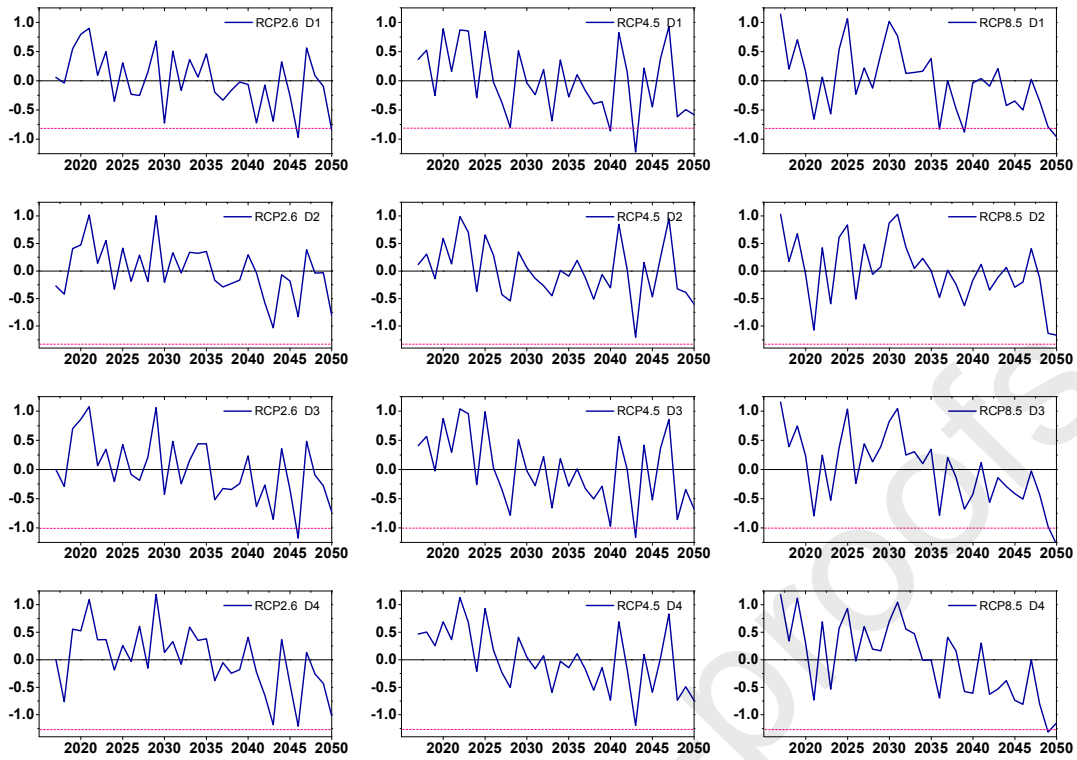

Fig. 11 Identification of future drought events that reduces crop yield for the four specified districts. The red dash line represents the critical point of SPEI ($SPEI_c$), below which are years that climatic factors significantly decrease crop yield.

Table 1 Climate models used in this study.

ID	*GCMs*	*Modeling Group*	*Country*
1	GFDL-CM3	NOAA Geophysical Fluid Dynamics Laboratory	USA
2	IPSL-CM5A-MR	Institut Pierre-Simon Laplace	France
3	MIROC5	Atmosphere and Ocean Research Institute (The University of Tokyo)	Japan
4	MRI-CGCM3	Meteorological Research Institute	Japan

Table 2 Correlation between crop yield and drought indices with different temporal scales.

Correlation	SPI1	SPI3	SPI12	SPEI1	SPEI3	SPEI12
Dingxin	-0.245	-0.316	-0.270	0.256	0.206	0.385
Dunhuang	-0.234	-0.265	0.373	0.373	0.414*	0.431
Gaotai	-0.042	0.006	-0.179	0.307	0.301	0.351
Guazhou	0.143	0.139	0.195	0.557**	0.473*	0.584**
Jiuquan	0.016	0.182	-0.100	0.204	0.278	0.276
Mazongshan	-0.244	0.275	-0.203	0.390	0.388	0.402*
Minqin	0.419	0.420*	0.448	0.522**	0.517*	0.561**
Shandan	0.275	0.400	0.345	0.236	0.319	0.248
Wushaoling	0.367*	0.310	0.360	0.222	0.361	0.407*
Wuwei	0.238	0.454*	0.489*	-0.346	0.534*	-0.555*
Yongchang	0.369*	0.522**	0.441*	0.428*	0.528**	0.550**
Yumenzhen	0.374	0.358	-0.369	0.428*	0.437**	0.388*
Zhangye	-0.368	-0.383	-0.368	0.525**	0.544**	0.447*
Hexi Region	-0.243	0.338	-0.296	0.351	0.399	0.420*

*indicates the correlation is significant at $p<0.05$ significance level

**indicates the correlation is significant at $p<0.01$ significance level

Declaration of interests

☒ The authors declare that they have no known competing financial interests or personal relationships that could have appeared to influence the work reported in this paper.

☐The authors declare the following financial interests/personal relationships which may be considered as potential competing interests:

Highlights:

- Drought evolutions in the Hexi Corridor for the last four decades were analyzed using SPI and SPEI
- The 12-month SPEI was the most relevant for the observed changes in climate yield
- The critical point of each SPEI-climatic yield curve was found for the four selected districts
- The crisis of the crop production corresponding to the future drought events are estimated